Hindawi Publishing Corporation
International Journal of Navigation and Observation
Volume 2011, Article ID 769264, 8 pages
doi:10.1155/2011/769264

Research Article

Lower Troposphere Observation over Urban Area with Lidar at 1064 nm

Atanaska Deleva and Ivan Grigorov

Institute of Electronics of the Bulgarian Academy of Sciences, 72, Tzarigradsko Chaussee Boulevard, 1784 Sofia, Bulgaria

Correspondence should be addressed to Atanaska Deleva, adeleva@ie.bas.bg

Received 18 July 2011; Revised 27 September 2011; Accepted 28 September 2011

Academic Editor: Nicolas Sifakis

An episode of relatively thick (till ~3 km) aerosol formation over the urban area of Sofia city was observed by lidar at a wavelength of 1064 nm. The lidar is part of Sofia lidar station at the Institute of Electronics of Bulgarian Academy of Sciences. Analysis of the weather conditions during the measurement period explains the stable persistence of such formation of human-activity aerosol over the town for the days of observation 20, 21, 23, and 24 June, 2011. The estimated top of the Planetary Boundary Layer for the measurement dated 23 June showed unusually high altitude ~2200 m above ground. The results are presented in terms of vertical atmospheric backscatter coefficient profiles and color maps of the aerosol stratification evolution.

1. Introduction

Aerosols are of central importance for global climate, atmospheric chemistry and physics, hydrological cycle and biosphere, ecosystems, and public health. Due to their short lifetime and strong tropospheric interactions, their global concentrations and properties are poorly known [1]. Aerosol particles affect atmospheric radiation and cloud microphysics and are considered a major uncertainty in climate changes. The term "atmospheric aerosol" encompasses a wide range of particle types having different compositions, sizes, shapes, and optical properties. Aerosols may be liquid or solid particles suspended in the air with typical diameters ranging over four orders of magnitude (approximately from a few nanometers to a few tens of micrometers). They consist of inorganic and organic components and varying amounts of water. Atmospheric particles are emitted from a variety of natural and human processes. On a global basis, the bulk of aerosols originate from natural sources, mainly sea salt, desert and soil dust, wildfire smoke, and volcanic ash [2, 3]. At present, the quantity of anthropogenic emissions increases with alarming speed. This is associated with a growing economy, rapid urban expansion, increasing rate of motorization, expanding industrial activity, and so forth. Human-produced particles can be dominant form of aerosol in highly populated and industrialized regions and in areas of intense agricultural burning. They are also tightly linked to problems of visibility reduction, acid rain, and smog in many industrial areas of the world. Anthropogenic aerosols are transported by prevailing winds, and the elements contained in them are redeposited often on the surface of the Earth far away from the location that they were produced [4–8].

The natural background aerosol is present in the absence of human activity, while the urban aerosol is dominated by anthropogenic sources. Urban aerosols have been identified as important factor impacting human health and the environment. Urban air consists of a significant fraction of submicrometer and ultrafine particles, which give a small contribution to the particulate mass, but are said to be associated with a number of significant negative impacts on human health. Smog is a type of air pollution derived from vehicular emission and from internal combustion engines and industrial fumes that react in the atmosphere under the sunlight influence. Smog can form in almost any climate, where industries or cities release large amounts of air pollutions. During periods of sunny weather, when the upper air is warm enough to inhibit vertical circulation in the atmosphere, the smog resides for a longtime near the ground, over densely populated cities or urban areas, and can build up to dangerous levels [9–12]. Such phenomena is often observed in geologic basins encircled by hills or mountains.

Actually, the physical and optical properties of atmospheric particles represent object of study aimed to understand more precisely the different influences of aerosols on the environment. Investigations are based on in situ measurements, lidar monitoring, and satellite imaging and often are organized as observational networks. However, despite recent advances in these efforts, there is a large uncertainty related mainly to the fact that the distribution and concentration of aerosols are highly variable both in space and time. The LIDAR (light detection and ranging) is an active remote sensing technique, because it uses laser light for the retrieval of atmospheric parameters. The lidar produces profiles of the reflected laser radiation at different wavelengths from the atmospheric components, gases, aerosols, and clouds. This is a well-established optoelectronic system for measuring trace atmospheric constituents, structure and dynamics, and clouds and also meteorological parameters, such as temperature, humidity, and wind velocity. Major advantage of lidar is the real-time observation of aerosol layering with high spatial and temporal resolution. That is the reason why lidars are increasingly confirmed as the best technique to capture individual atmospheric events and integrate them into regional or global pictures of the aerosol transport and stratification. The largest aerosol research project in Europe is EARLINET (European Aerosol Research Lidar Network). It started in 2000, with the primary objective to provide a comprehensive, quantitative, and statistically significant data base for aerosol distribution on a continental scale [13, 14]. EARLINET is a coordinated network of lidar stations that uses advanced methods for vertical profiling of aerosols. In March, 2003, Bulgarian lidar station at Sofia was involved in systematic measurements on a regular basis three times per week according to the schedule of the EARLINET project.

In this study, we report an observation on the vertical distribution of a relatively stable aerosol layer over Sofia city, Bulgaria. The lidar measurements are performed on no-Saharan-dust-affected days; therefore, we infer that a smog loading in the air was detected. The observed layer persisted in the atmosphere from the ground up to 3 km in the period 20–24 June, 2011.

2. Experimental Site, Lidar System, and Data Processing

The single lidar station in Bulgaria is positioned in Sofia, in the Laser Radar Laboratory of the Institute of Electronics of Bulgarian Academy of Sciences (IE-BAS). The Institute is located in the urban area of the capital Sofia (42°39′14″N, 23°23′14″E), at about 550 m above sea level (ASL), nearby the main road connecting Europe and the Middle East, in a natural basin supported by mountains. The highest range is situated at the South-West of the valley immediately above Sofia and corresponds to Vitosha Mountain (its peak Cherni Vruh is 2290 m high).

Sofia lidar station has two functional lidars. The first one is based on a CuBr-vapor laser, and the other one—on Nd:YAG laser. The investigation presented in this work is accomplished using the channel at 1064 nm for elastic backscatter of the lidar with Nd:YAG laser. This lidar is presented in details in previous publications [15, 16]; therefore, only brief description of its setup is given below. Recently, a ground-based 3-channel lidar was developed in the Laser Radar Lab. It is configured in a monostatic biaxial alignment pointing at angle 32° with respect to the horizon, as determined by its disposition in the lab. Therefore, despite signals from as far as 30 km distance are recorded, the maximum sounding height is limited to 16 km. The radiation source is a Q-switched frequency-doubled Nd:YAG laser (pulse energy: up to 600 mJ at 1064 nm, 80 mJ at 532 nm; fixed repetition rate 2 Hz) provided with a single-pass optical amplifier. Laser light backscattered by the atmosphere is received by a Cassegrain telescope (aperture: 35 cm; focal distance: 200 cm). The output beam from the telescope is passed to the spectrum analyzer for spectral separation of the incoming optical signals. The wavelength separator consists of three selective spectral channels for 1064 nm, 532 nm, and 607 nm (the Raman shift wavelength of nitrogen molecules with respect to the one of the sounding laser radiation at 532 nm). Data acquisition system includes newly developed hardware and software components, specialized in accomplishing the lidar measurement and data processing. The hardware components have been designed as an integrated photoreceiver modules consisting of photoreceiving sensor, controlled photoreceiver power supply, amplifier, 14-bit analog-to-digital converter (ADC), and USB-interface for computer connection. Distinguishing features of the photoreceiver modules are high sensitivity, high amplification factor, low noise level, low power consumption, small dimensions, and weight. The modules differ only in photoreceiving sensors used, resulting from the substantial differences in wavelength and power of the received signals.

The data acquisition software contains two main programs and several auxiliary ones. The first main program is designed for real-time control of the lidar system during measurements and displaying lidar profiles at each laser pulse or after averaging and to save data. Received signals are digitized every 100 ns with an ADC, resulting in a 15 m range resolution (about 7.5 m altitude resolution). Thus, the lidar measures the temporal evolution of atmospheric aerosol backscatter with high time and range resolution. The second main program is a package providing the calculation of the atmospheric backscatter coefficient and determination of the error in the estimates. The well-known Klett-Fernald's [17–19] inversion algorithm is used in these retrievals. Since the magnitude of the backscatter coefficient value is proportional to the aerosol density, the changes of the calculated profiles in time and space illustrate the temporal evolution and stratification of the aerosols in the air over the lidar station.

3. Results and Comments

The lidar observation covered a period of about a week during the second half of June, 2011. We present below measured profiles of the atmospheric aerosol backscatter coefficient at wavelength 1064 nm for 20, 21, 23, and 24 June. As mentioned, the laser beam propagated at angle

of 32° to the horizon, and the raw space resolution of 15 m was converted to ~7.9 m in height. Therefore, the maximal altitude of the measurements reached a range of 16 km above ground level (AGL). We used Klett-Fernald inversion starting from such altitude with the assumption of only molecular backscattering, with known values retrieved from the model of Standard atmosphere. The lidar signal was accumulated for 5 min of averaging time. Subsequently, these profiles are summarized to cover one hour time of observation. So, the calculated backscatter coefficient profiles represent averaged for one-hour profiles of the atmospheric backscatter coefficient. A constant lidar ratio with value of 45 sr [20] was used in the calculations. We assumed the relative uncertainty of the retrieved values of aerosol backscatter coefficient in order of 11% at altitude 3.0–3.5 km AGL, as it was estimated for Sofia lidar station in the internal algorithm quality check for EARLINET lidars [21].

Below, we also present maps of the time evolution of aerosol stratification build on the basis of the so-called range corrected signal (RCS). RCS is produced by subtracting the estimated background noise from the raw lidar signal and multiplying by the square of the distance to the backscattering atmospheric sample. Presented in the work, maps of RCS evolution over Sofia lidar station are freely accessible on the WEB-page of IE-BAS [22]. These maps show in general changes of the aerosol stratification over the lidar station during the measurement period. The original 5 min duration profiles were used to convert lidar signal amplitudes to appropriate colors; that is, the time resolution of each map is 5 min. At the base of the RCS gradient over height, the top limit of the atmospheric planetary boundary layer (PBL) was calculated. The PBL is the lower layer of the atmosphere, where in practice are cumulated most of the aerosols originating from human activities. Its top limit marks the height of the convection process due to the diurnal cycle of worming and cooling of the Earth surface.

To describe the meteorological situation over the area of Sofia (and Bulgaria), we used the weather forecast maps elaborated by Barcelona Supercomputing Center (BCS) for Euro-Mediterranean zone [23]. These maps give an image of the wind direction and speed, position of cloud fields, and magnitude of dust load in the atmosphere above North Africa and Europe. Referring to the maps for the days of lidar measurements, presented on Figure 1, it was evident that Bulgaria resided far from Sahara dust circulation. Also, the cloud formations pass in the north of the Balkans. Briefly, clear sky, without noticeable aerosol layers should be expected in lidar observation.

Valuable information about the origin and path that the observed air-mass passed before arrival over the lidar site we obtained from the HYSPLIT (HYbrid Single-Particle Lagrangian Integrated Trajectory) model [24, 25]. It represents a complete system for computing simple air parcel trajectories to complex dispersion and deposition simulations. The model can be run interactively on the Web through the READY system [3, 4] available on the website of Air Resource Laboratory of NOAA (National Oceanic and Atmospheric Administration), USA. The maps of the calculated backward air masses trajectories are presented on Figure 2. We used 5-day interval to follow the movement of air masses before they arrive over Sofia at three altitudes 1000 m, 2000 m, and 3000 m AGL. These altitudes are chosen in view of the observed aerosol stratification in our lidar measurements.

The results of lidar measurements are presented on the following four figures.

In Figure 3 are shown the results of lidar measurement on 20 June, 2011. The measurement starts at 09:15 h UTC and stops at 17:55 h UTC in the afternoon, with a pause from 11:15 h to 15:56 h UTC in mid-time. Four profiles of the atmospheric backscatter coefficient are retrieved. An aerosol layer was observed in the morning at altitude 1500 m to 3000 m AGL. Consulting the plot of backward air masses trajectories corresponding to the morning-time measurement (Figure 2(a)) an upward advection till altitude of 3 km AGL of hot air and ground aerosols can be seen, marked by the lower trajectory in the last ~30 hours before the end point over Sofia. The higher colder air masses, originating from North Atlantic, encounter the rising warm and humid Mediterranean air near the lidar site. Therefore, we assumed that the aerosol layer observed at 1.5–3 km was a residual layer, formed by water vapor flooding of small quantities of aerosol during sunrise and shortly after. It was imperceptible by eye but clearly noticeable for the light at 1064 nm wavelength. The aerosol layer disappears at mid-day and was no longer observed in the afternoon, when the Earth surface was already warm. The plot of backward trajectories, finishing above Sofia at 17:00 UTC (Figure 2(b)), shows semilaminar path of the air masses from different height. Active advection processes are present away from the lidar site, so only high PBL is observed in the afternoon. The points on the graphics of the aerosol backscatter coefficient profiles (Figure 3(a)) mark the estimated top limits of PBL for each measurement interval. A monotonic increase of this limit was observed during the entire day: 1080 m AGL for the first hour of measurement, at 09:15 h UTC, 1170 m AGL—at 10:15 h UTC, 1400 m AGL—at 15:56 h UTC and 1700 m AGL—at 16:55 h UTC. The hot weather, during the week of lidar observation, should be the cause of such behavior of the PBL top limit, without decrease of the height in the afternoon and evening. As a consequence, unusually high aerosol boundary layer (near the Earth surface) was observed till altitudes ~3 km AGL. The calculated values of the aerosol backscatter coefficient were $\sim 8.6 \times 10^{-6}\,\mathrm{sr}^{-1}\,\mathrm{m}^{-1}$ near the ground and $\sim 8.3 \times 10^{-7}$–$4.5 \times 10^{-7}\,\mathrm{sr}^{-1}\,\mathrm{m}^{-1}$ at the estimated top of PBL. As neither other source of aerosols, nor dust transport from Sahara over the Mediterranean was forecasted for this period, our conclusion was that the smog of human activities and traffic in town caused the observed aerosol stratification.

In Figure 4, the results of lidar measurement on 21 June, 2011 are shown. The measurement starts at 08:30 h UTC and stops at 11:27 h UTC at noon. Three profiles of the atmospheric backscatter coefficient are retrieved each averaged for 1 hour interval. The estimated top limit of the PBL for the time of measurement resides constant at ~1500 m AGL. Backscatter aerosol profiles similar to the ones illustrated in Figure 3 were observed, with unusually

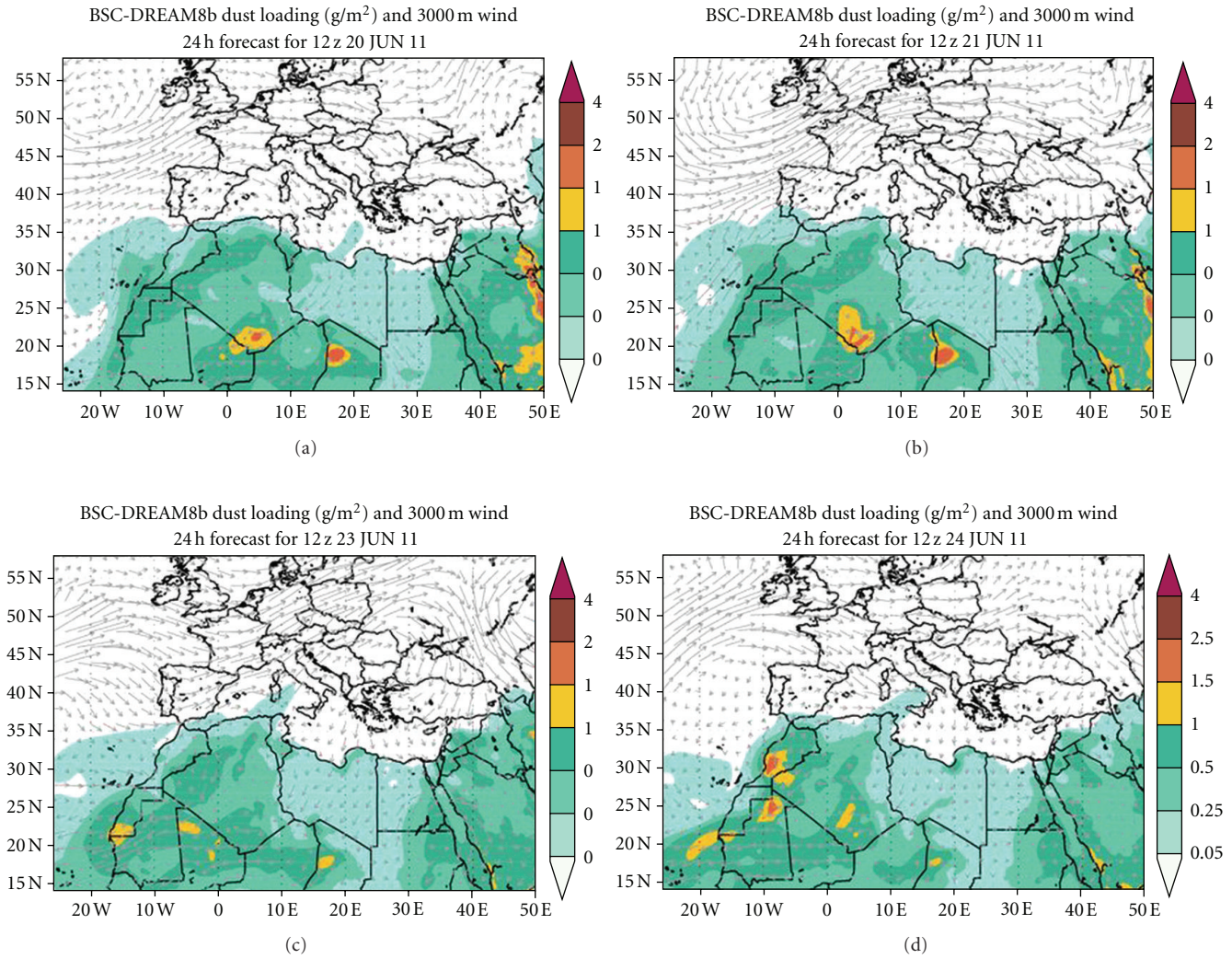

Figure 1: Forecast map of Sahara dust load in the atmosphere, provided by Barcelona Supercomputing Center (BCS) for the four days of lidar measurements: (a) 20 June, 2011, (b) 21 June, 2011, (c) 23 June, 2011, and (d) 24 June, 2011.

high aerosol boundary layer reaching altitude ~2–2.2 km. The map of the backward air masses trajectories (Figure 2(c)) indicates a habitual atmospheric movement over Sofia, without sudden motion either horizontally, or vertically. The forecast map (Figure 1(b)) shows no dust transport from Sahara. The boundary aerosol layer remains stable during the 3-hour time interval of observation, with calculated values of the backscatter coefficient in the range of 8.5×10^{-6} sr^{-1} m^{-1} near the ground and 3.6×10^{-7} sr^{-1} m^{-1}at the estimated top of PBL.

In Figure 5, the results of lidar measurement on 23 June, 2011 are presented. The measurement starts at 07:27 h UTC in the morning and stops at 17:59 h UTC in the afternoon with a pause about noon time from 10:25 h to 15:59 h UTC. Five profiles of the atmospheric backscatter coefficient are retrieved each averaging 1 hour interval. The height of the estimated top limit of PBL for the measurements in the morning increased slightly from 1100 m AGL to 1280 m AGL, which was normal considering Earth surface warming. For the afternoon measurements, the estimated heights of the top of PBL reached unusual values of 2200 m AGL at 15:59 h UTC, and 2300 m AGL at 16:59 h UTC. The backward trajectories for the measurements in the morning and in the afternoon (Figures 2(d) and 2(e) show a transport of cold air parcels that arrive over Sofia at altitude above 2 km (trajectories in blue and green color)). Third trajectory changes a little the direction last day before reaching the lidar site from East to South-East, traversing wormer regions. It was sufficient for the air to be warmed enough to rise higher than in the morning and to extend the top of PBL to greater values. Likewise during the previous measurements on 20 and 21 June, an unusually high aerosol boundary layer, reaching altitude ~3 km AGL, was observed. The calculated aerosol backscatter values were ~9.03×10^{-6} sr^{-1} m^{-1} near the ground and 8.3×10^{-7}–4.0×10^{-7} sr^{-1} m^{-1}at the estimated top of PBL. The heat and the lack of winds in the valley, where Sofia is located, caused elevation of the city smog to such unusual heights.

The results of lidar measurement on 24 June, 2011 are presented in Figure 6. The measurement starts at 07:52 h

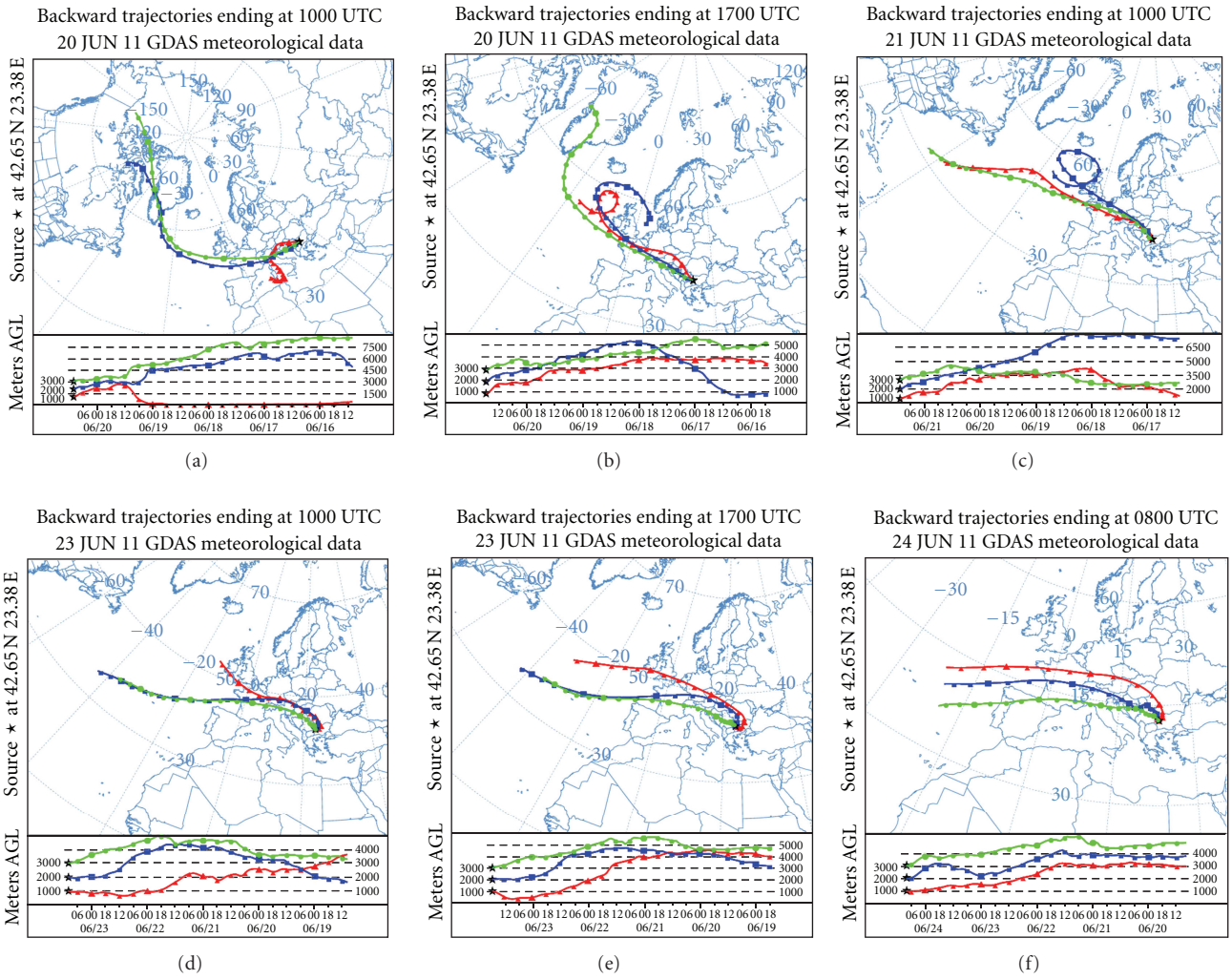

FIGURE 2: Backward air-mass trajectories, calculated using HYSPLIT model. They show the origin and the way of air mass 5 days before arrival over the site of lidar observation.

UTC and stops at 09:22 h UTC in the morning. Three profiles of the atmospheric backscatter coefficient are retrieved each averaged for 30 min interval. The height of the estimated top limit of the PBL remains constant with value of ~700 m AGL for all measurements. This value was normal for summer time for the region. The calculated aerosol backscatter values were $\sim 9.88 \times 10^{-6}\,\mathrm{sr}^{-1}\,\mathrm{m}^{-1}$ near the ground and $\sim 1.2 \times 10^{-6}\,\mathrm{sr}^{-1}\,\mathrm{m}^{-1}$ at the estimated top of PBL. The backscatter aerosol profiles above the top limit of the PBL show relatively bigger than usual constant values till altitudes of 2200 m–2500 m AGL in the range of $6.5 \times 10^{-7}\,\mathrm{sr}^{-1}\,\mathrm{m}^{-1}$ at altitude 1 km AGL and $2.0 \times 10^{-7}\,\mathrm{sr}^{-1}\,\mathrm{m}^{-1}$ at 2 km AGL. That shows again an increased smog load in the low troposphere due to human activity and the specific weather conditions. As it is evident from the plot of backward trajectories (Figure 2(f)), the air masses move semihorizontally, slowing its movement near Sofia that results in relatively stable atmospheric aerosol stratification. Time evolution of the aerosol layers is presented on Figure 6(b), illustrating their invariability during the lidar observation.

4. Conclusions

In this work are presented the results of lidar measurements at wavelength 1064 nm, performed from 20 to 24 June, 2011 in Sofia, Bulgaria. An episode of relatively thick aerosol aggregation, just above the Earth's surface, over the urban area of Sofia city was observed. On 23 June, 2011, in the afternoon, an unusually high for the region, top of PBL at altitude of 2200 m AGL was estimated using the lidar data. Calculated values of aerosol backscatter coefficient were about 8.5–9.0 $\times$ $10^{-6}\,\mathrm{sr}^{-1}\,\mathrm{m}^{-1}$ near the ground and 3.0–3.2 $\times$ $10^{-7}\,\mathrm{sr}^{-1}\,\mathrm{m}^{-1}$ at the estimated tops of PBL for the different measurements. Elevated values of the aerosol backscatter coefficient were calculated for altitudes above PBL, till ~3 km AGL. Backward trajectories analysis and Sahara dust forecast maps outline in general the meteorology and justify the results of lidar measurements. The specific weather conditions during the period of lidar measurements—extreme heat and lack of wind—caused the stable persistence of this aggregation for all 4 days of observation.

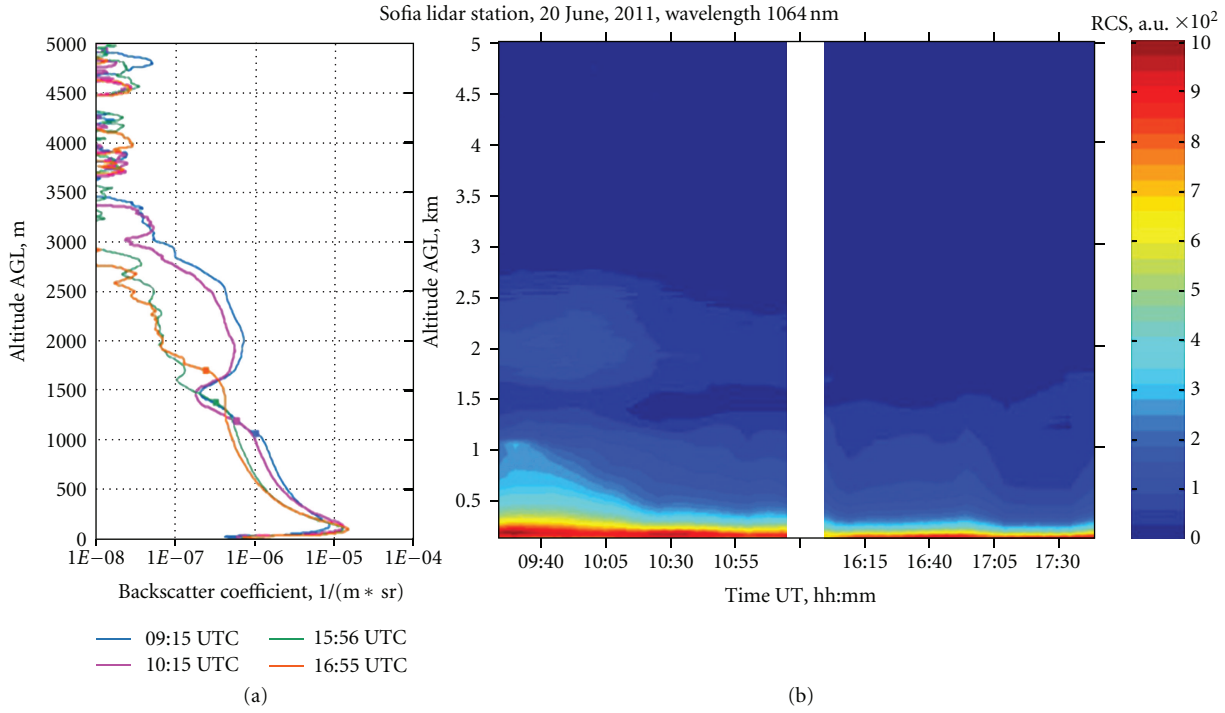

Figure 3: Backscatter coefficient profiles (a) and map of the aerosol stratification (b) measured on 20 June, 2011. Four backscatter profiles are presented, each averaged for one hour time of measurement. The marks on the profiles show the estimated height of the upper limit of the planetary boundary layer (PBL). In morning time, a well-distinguished aerosol layer is observed at 1500 to 3000 m altitude AGL.

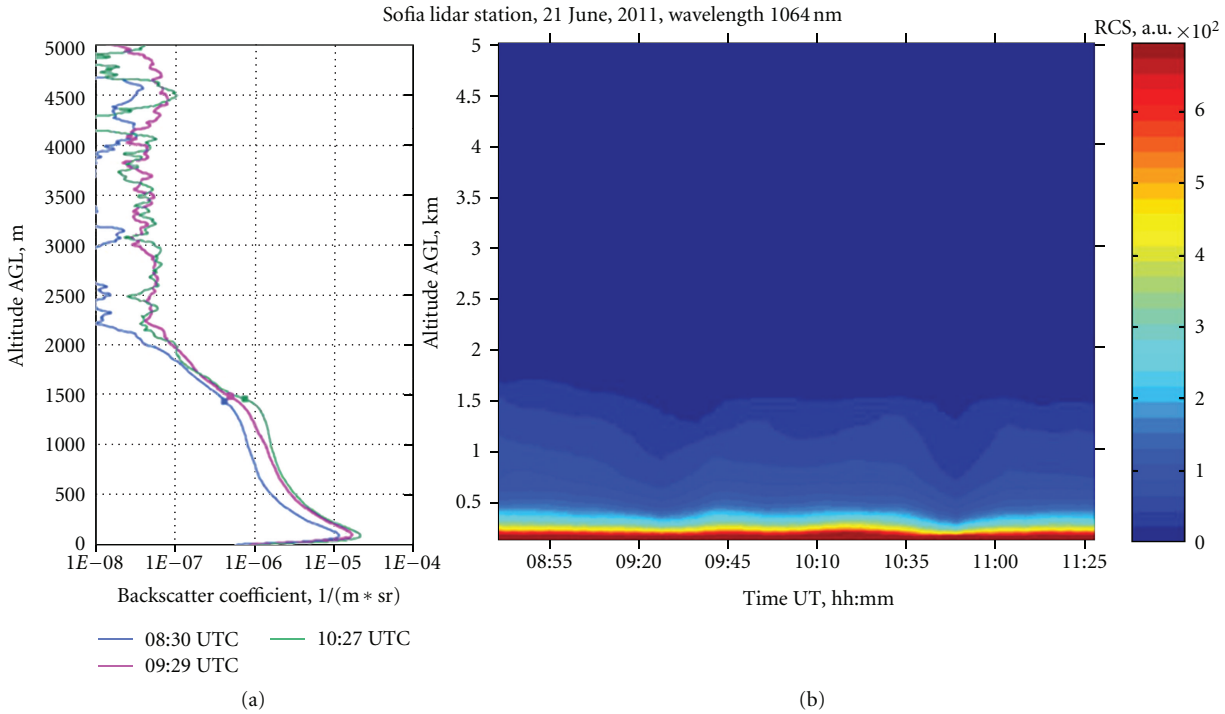

Figure 4: Backscatter coefficient profiles (a) and map of the aerosol stratification (b) measured on 21 June, 2011. The averaging time for each backscatter profile is one hour. The marks show the estimated height of the upper limit of the PBL.

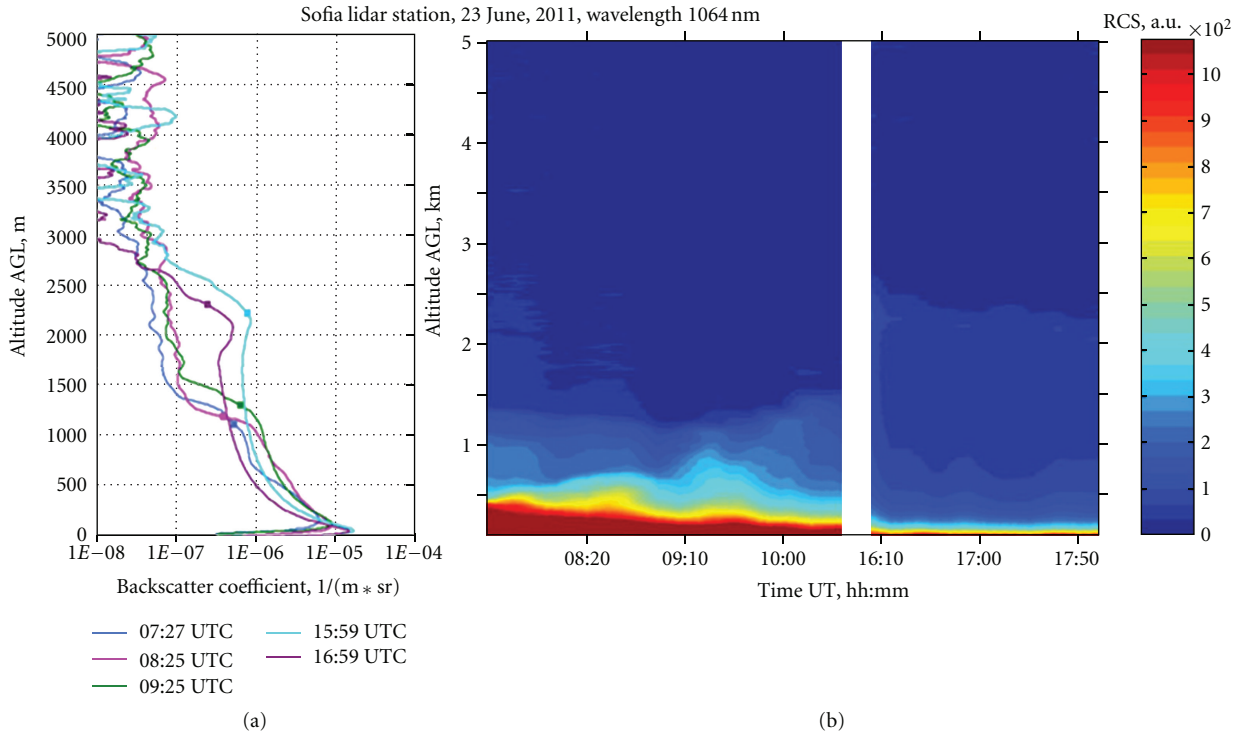

Figure 5: Backscatter coefficient profiles (a) and map of the aerosol stratification (b) measured on 23 June, 2011. On the graphs of the averaged for one-hour aerosol backscatter profiles are marked the estimated upper limits of the PBL.

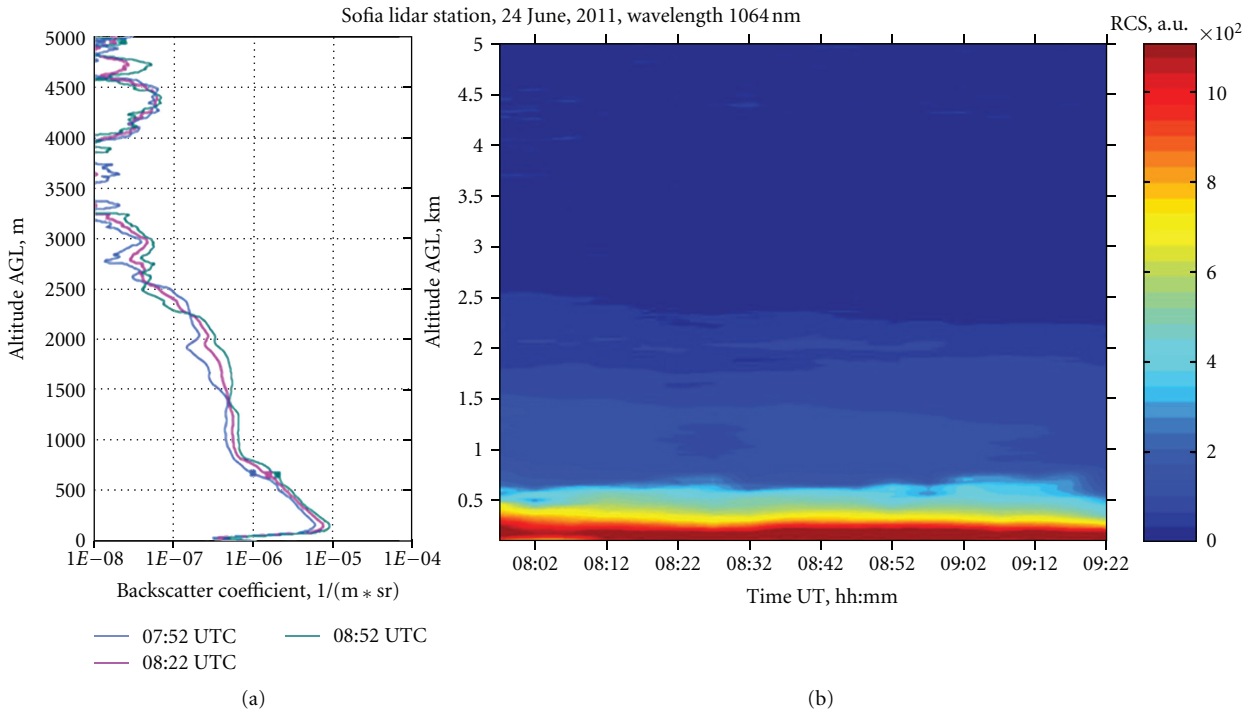

Figure 6: Backscatter coefficient profiles (a) and map of the aerosol stratification (b) measured on 24 June, 2011. The estimated upper limits of the PBL are marked with points on the graphs of the averaged for half-an-hour aerosol backscatter profiles.

Acknowledgments

This work is supported by the project of FP7 "Aerosols, Clouds, and Trace gases Research Infrastructure Network" (ACTRIS), INFRA-2010-1.1.16. The authors gratefully acknowledge the NOAA Air Resources Laboratory (ARL) for the provision of the HYSPLIT model for air masses transport and dispersion and/or READY website used in this paper. The authors would like also to express their gratitude to the Earth Sciences Division, Barcelona Supercomputing Center, Spain, for the provision of the DREAM model aerosol dust data used in this paper.

References

[1] P. Forster et al., "Contribution of working group I to the fourth assessment report of the intergovernmental panel on climate change," in *Climate Change 2007: The Physical Science Basis*, S. Solomon, D. Qin, M. Manning et al., Eds., Cambridge University Press, New York, NY, USA, 2007.

[2] J. Gasteiger, S. Großß, V. Freudenthaler, and M. Wiegner, "Volcanic ash from Iceland over Munich: mass concentration retrieved from ground-based remote sensing measurements," *Atmospheric Chemistry and Physics*, vol. 11, no. 5, pp. 2209–2223, 2011.

[3] A. Papayannis, V. Amiridis, L. Mona et al., "Systematic lidar observations of Saharan dust over Europe in the frame of EARLINET (2000–2002)," *Journal of Geophysical Research D*, vol. 113, no. 10, Article ID D10204, 17 pages, 2008.

[4] J. E. Penner et al., "Contribution of working group I to the third assessment report of the intergovernmental panel on climate change," in *Climate Change 2001: The Physical Scientific Basis*, B. Nyenzi and J. Prospero, Eds., Cambridge University Press, Cambridge, UK, 2001.

[5] U.S. Climate Change Science Program, "Aerosol properties and climate impacts," in *Synthesis and Assessment Product*, M. Chin, R. Kahn, and S. Schwartz, Eds., 2009, http://downloads.climatescience.gov.

[6] U. Pöschl, "Atmospheric aerosols: composition, transformation, climate and health effects," *Angewandte Chemie*, vol. 44, no. 46, pp. 7522–7540, 2005.

[7] P. Stier, J. Feichter, E. Roeckner, S. Kloster, and M. Esch, "The evolution of the global aerosol system in a transient climate simulation from 1860 to 2100," *Atmospheric Chemistry and Physics*, vol. 6, no. 10, pp. 3059–3076, 2006.

[8] R. L. Miller and I. Tegen, "Climate response to soil dust aerosols," *Journal of Climate*, vol. 11, no. 12, pp. 3247–3267, 1998.

[9] N. Sabbagh-Kupelwieser, H. Horvath, and W. W. Szymanski, "Urban aerosol studies of PM1 size fraction with reference to ambient conditions and visibility," *Aerosol and Air Quality Research*, vol. 10, no. 5, pp. 425–432, 2010.

[10] E. Katragkou, S. Kazadzis, V. Amiridis, V. Papaioannou, S. Karathanasis, and D. Melas, "PM10 regional transport pathways in Thessaloniki, Greece," *Atmospheric Environment*, vol. 43, no. 5, pp. 1079–1085, 2009.

[11] M. Tasić, S. Rajšić, Z. Mijić et al., "Atmospheric aerosols and their influence on air quality in urban areas," *Facta Universitatis*, vol. 4, pp. 83–90, 2006.

[12] L. Perez, A. Tobias, X. Querol et al., "Coarse particles from saharan dust and daily mortality," *Epidemiology*, vol. 19, no. 6, pp. 800–807, 2008.

[13] EARLINET (European Aerosol Research Lidar Network), http://www.earlinet.org/.

[14] S. Guibert, V. Matthias, M. Schulz et al., "The vertical distribution of aerosol over Europe—synthesis of one year of EARLINET aerosol lidar measurements and aerosol transport modeling with LMDzT-INCA," *Atmospheric Environment*, vol. 39, no. 16, pp. 2933–2943, 2005.

[15] A. Deleva, A Slesar, and S. Denisov, "Investigations of the aerosol fields and clouds in the troposphere with Raman-aerosol lidar," *Bulgarian Geophysical Journal*, vol. 36, pp. 25–39, 2010.

[16] A. D. Deleva, I. V. Grigorov, L. A. Avramov, V. A. Mitev, A. S. Slesar, and S. Denisov, "Raman-elastic-backscatter lidar for observations of tropospheric aerosol," in *Proceedings of 15th SPIE International Scool on Quantum Electronics: Lasers-Physics and Applications*, vol. 7027, pp. 70270Y-1–70270Y-8, 2008.

[17] J. D. Klett, "Stable analytical inversion solution for processing lidar returns," *Applied Optics*, vol. 20, no. 2, pp. 211–220, 1981.

[18] F. G. Fernald, "Analysis of atmospheric lidar observations: some comments," *Applied Optics*, vol. 23, pp. 652–653, 1984.

[19] Y Sasano, E. Browell, and S. Ismail, "Error caused by using constant extinction/backscattering ratio in the lidar solution," *Applied Optics*, vol. 24, pp. 3929–3932, 1985.

[20] J. Boesenberg and V. Matthias, "A European aerosol research lidar network to establish an aerosol climatology," MPI-Report 348, Max-Planck-Institut für Meteorologie, Hamburg, Germany, 2003.

[21] C. Böckmann, U. Wandinger, A. Ansmann et al., "Aerosol lidar intercomparison in the framework of the EARLINET project. 2. Aerosol backscatter algorithms," *Applied Optics*, vol. 43, no. 4, pp. 977–989, 2004.

[22] Quicklooks of Sofia lidar station, http://www.ie-bas.dir.bg/Departments/LidarData/Quicklooks.htm.

[23] DREAM (Dust Regional Atmospheric Model) model access via Barcelona Supercomputing Center, http://www.bsc.es/projects/earthscience/DREAM.

[24] R. R. Draxler and G. D. Rolph, HYSPLIT (HYbrid Single-Particle Lagrangian Integrated Trajectory) Model access via NOAA ARL READY Website. NOAA Air Resources Laboratory, Silver Spring, MD, http://ready.arl.noaa.gov/HYSPLIT.php/.

[25] G. D. Rolph, Real-time Environmental Applications and Display sYstem (READY). NOAA Air Resources Laboratory, Silver Spring, MD, http://ready.arl.noaa.gov/.